The Effects of Rosiglitazone on Insulin Sensitivity, Lipolysis, and Hepatic and Skeletal Muscle Triglyceride Content in Patients With Type 2 Diabetes

Adam B. Mayerson,[1] Ripudaman S. Hundal,[1] Sylvie Dufour,[1,3] Vincent Lebon,[1,3] Douglas Befroy,[1,3] Gary W. Cline,[1] Staffan Enocksson,[1] Silvio E. Inzucchi,[1] Gerald I. Shulman,[1,2,3] and Kitt F. Petersen[1]

We examined the effect of three months of rosiglitazone treatment (4 mg b.i.d.) on whole-body insulin sensitivity and in vivo peripheral adipocyte insulin sensitivity as assessed by glycerol release in microdialysis from subcutaneous fat during a two-step (20 and 120 mU · m^{-2} · min^{-1}) hyperinsulinemic-euglycemic clamp in nine type 2 diabetic subjects. In addition, the effects of rosiglitazone on liver and muscle triglyceride content were assessed by ^{1}H-nuclear magnetic resonance spectroscopy. Rosiglitazone treatment resulted in a 68% ($P < 0.002$) and a 20% ($P < 0.016$) improvement in insulin-stimulated glucose metabolism during the low- and high-dosage−insulin clamps, respectively, which was associated with ~40% reductions in plasma fatty acid concentration ($P < 0.05$) and hepatic triglyceride content ($P < 0.05$). These changes were associated with a 39% increase in extramyocellular lipid content ($P < 0.05$) and a 52% increase in the sensitivity of peripheral adipocytes to the inhibitory effects of insulin on lipolysis ($P = 0.04$). In conclusion, these results support the hypothesis that thiazolidinediones enhance insulin sensitivity in patients with type 2 diabetes by promoting increased insulin sensitivity in peripheral adipocytes, which results in lower plasma fatty acid concentrations and a redistribution of intracellular lipid from insulin responsive organs into peripheral adipocytes. *Diabetes* 51: 797–802, 2002

From the [1]Department of Internal Medicine, Yale University School of Medicine, New Haven, Connecticut; the [2]Department of Cellular and Molecular Physiology, Yale University School of Medicine, New Haven, Connecticut; and [3]Howard Hughes Medical Institute, Yale University School of Medicine, New Haven, Connecticut.

Address correspondence and reprint requests to Kitt F. Petersen, M.D., Department of Internal Medicine, Yale University School of Medicine, 333 Cedar St., Fitkin 1, Box 208020, New Haven, CT 06520-8020. E-mail: kitt.petersen@yale.edu.

Received for publication 3 October 2001 and accepted in revised form 31 October 2001.

S.E.I. has received honoraria and is on the speakers' bureau for both Glaxco/SmithKline and Takeda Pharmaceuticals America and has also received research support from Takeda. G.I.S. has served as a research consultant for Glaxo/SmithKline Beecham.

DEXA, dual-energy X-ray absorptiometry; EMLC, extramyocellular lipid content; GDR, glucose disposal rate; ETOH, ethanol; $ETOH_{in}$, ethanol concentration measured in the perfusate; $ETOH_{out}$, ethanol concentration in the dialysate; GCMS, gas chromatography−mass spectrometry; GIR, glucose infusion rate; GP, endogenous glucose production; IMLC, intramyocellular lipid content; NMR, nuclear magnetic resonance; PPAR-γ, peroxisome proliferator−activated receptor-γ; TNF-α, tumor necrosis factor-α; TZD, thiazolidinedione.

Although thiazolidinediones (TZDs) are now widely used to treat type 2 diabetes, their mechanism of action remains largely unknown. It has been well established that TZDs enhance insulin sensitivity by acting as ligands for the transcription peroxisome proliferator−activated receptor-γ (PPAR-γ) (1,2). However, PPAR-γ is predominantly expressed in adipose tissue, whereas the improvement in insulin sensitivity occurs predominately in skeletal muscle (3–5) where PPAR-γ expression is relatively low (1,2). This paradox suggests that the TZDs may indeed modulate key communication signals between fat and muscle, such as leptin (6), adiponectin (7), tumor necrosis factor-α (TNF-α) (8), resistin (9), and fatty acids (10–13). In support of fatty acids being an important factor in this regard, recent studies have demonstrated a strong relationship between tissue lipid content and insulin resistance in both skeletal muscle (14–20) and liver (15,16,21).

In this study, we examined the hypothesis that TZDs improve insulin sensitivity in patients with type 2 diabetes by promoting the redistribution of triglyceride from liver and muscle to peripheral adipocytes. In that regard, we analyzed the effects of rosiglitazone, a TZD, in subjects with type 2 diabetes using several different complementary methodologies. ^{1}H-nuclear magnetic resonance (NMR) spectroscopy was used to assess triglyceride content in liver and muscle in conjunction with the hyperinsulinemic-euglycemic clamp, and indirect calorimetry was used to assess insulin sensitivity. The effects of rosiglitazone on peripheral adipocyte lipolysis during the clamp were assessed by microdialysis measurements of glycerol release from subcutaneous fat.

RESEARCH DESIGN AND METHODS

Subjects. The participants in this study were nine nonsmoking healthy subjects with type 2 diabetes. Their clinical and metabolic profiles are detailed in Table 1. Generally, this was a middle-aged, obese group of patients with well-controlled diabetes. At the time of enrollment, six subjects were taking metformin, a sulfonylurea, or both, and the remaining three subjects were managing their diabetes with diet alone. Informed written consent was obtained from all subjects after the aims and potential risks of the study were explained to them. The protocol was approved by the Yale University School of Medicine Human Investigation Committee.

Study design. After a medical screening, a wash-out period of 10–14 days was allowed for the discontinuation of any prior oral antidiabetic regimen. For the 3 days before the start of the trial, subjects consumed a weight-maintenance diet according to the guidelines of the American Diabetes Association (60% carbohydrate, 20% protein, 20% fat), evenly divided among

TABLE 1
Anthropometric and fasting plasma metabolite concentrations before and after 3 months of rosiglitazone treatment

	Before	After	*P*
Body weight (kg)	92.3 ± 6.2	93.9 ± 5.7	0.34
BMI (kg/m^2)	31.1 ± 1.6	31.9 ± 1.7	0.20
Lean body mass (kg)	61.3 ± 3.4	59.9 ± 2.5	0.98
Body fat (%)	29.9 ± 3.6	33.1 ± 4.5	0.78
HbA_{1c} (%)	6.7 ± 0.4%	7.2 ± 0.6%	0.23
Plasma glucose (mmol/l)	9.0 ± 0.9	7.9 ± 0.9	0.02
Insulin (pmol/l)	93.6 ± 13.8	71.4 ± 7.8	0.03
C-peptide (pmol/l)	0.83 ± 0.08	0.76 ± 0.06	0.19
Glucagon (ng/l)	87.0 ± 9.0	83.2 ± 7.3	0.54
Total cholesterol (mmol/l)	4.97 ± 0.39	5.43 ± 0.41	0.09
HDL cholesterol (mmol/l)	0.88 ± 0.05	0.96 ± 0.05	0.15
LDL cholesterol (mmol/l)	2.92 ± 0.34	3.31 ± 0.21	0.14
Triglycerides (mmol/l)	6.31 ± 1.66	6.26 ± 1.34	0.97
Fatty acids (μmol/l)	497 ± 64	352 ± 55	0.003
Leptin (ng/ml)	21.1 ± 5.7	18.4 ± 4.7	0.34
Alkaline phosphatase (units/l)	72 ± 7	61 ± 7	0.007
γ-Glutamyl transpeptidase (units/l)	29 ± 6	17 ± 3	0.001

Data are means ± SE.

three meals Subjects were then admitted to the Yale/New Haven Hospital General Clinical Research Center, where they underwent a series of metabolic investigations. After these baseline studies, subjects took rosiglitazone (4 mg b.i.d., p.o.) for 10–12 weeks. The subjects were then readmitted to the center and underwent the identical metabolic investigations conducted during the baseline evaluation. During the treatment period, subjects were evaluated every 2 weeks to ensure compliance and to assess them for adverse events, including liver dysfunction.

Insulin clamp procedure. At 8:00 A.M., a 3-h primed (corrected for ambient fasting plasma glucose level), continuous infusion of [6,6-^{2}H]glucose (2 mg · m^{-2} body surface area · min^{-1}) and [1,1,2,3,3-$^2H_5$]glycerol (~0.02 mg · m^{-2} body surface area · min^{-1}) were begun through an antecubital vein. During the third hour of infusion, a retrograde cannula was inserted into a vein in the contralateral hand, which was warmed for the sampling of arterialized venous blood. A small volume of 0.9% NaCl flowed through the sampling cannula to maintain patency. Blood samples were withdrawn at 10-min intervals during the final 40 min of the third hour for the measurement of plasma glucose and insulin levels and glucose isotope enrichment. After 3 h of isotope infusion, a two-step hyperinsulinemic-euglycemic clamp was initiated, as previously described (3). During the first step, a low dosage of insulin was infused at 20 mU · m^{-2} · min^{-1} for 120 min to assess insulin's effects on peripheral adipocyte lipolysis. During the second step, a high dosage of insulin was infused at 120 mU · m^{-2} · min^{-1} for 240 min to assess insulin's effects on peripheral glucose disposal and suppression of endogenous glucose production.

Indirect calorimetry. During the final 30 min of the basal infusion and each step of the insulin clamp, indirect calorimetry was performed using the ventilated hood technique (Deltatrack Metabolic Monitor, Sensorimedics, Anaheim, CA) to measure basal fasting rates of glucose and lipid oxidation, as previously described (22).

Adipose tissue microdialysis. The microdialysis probe (CMA/60; CMA, Microdialysis, Solna, Sweden) and details of the microdialysis experiments have been previously described (23,24). Briefly, a dialysis tubing (20-mm shaft, 30-mm membrane, 20 kDa) was attached to the end of double-lumen polyurethane tubing. The perfusate entered through the outer lumen, flowed to the microdialysis membrane, and was subsequently collected (dialysate) throughout the outer lumen. Once steady state was reached, the composition of the dialysate reflected that of the interstitial fluid (25). After an overnight fast, and before the baseline infusions were begun for the insulin clamp, two dialysis probes were inserted percutaneously into the subcutaneous tissue of the abdomen, 4–6 cm lateral to the umbilicus. To estimate regional adipose tissue blood flow, a microdialysis ethanol technique was used, as previously described and validated (26,27). Briefly, an ethanol-based perfusate (50 mmol/l) was infused through each probe using a microinjection pump (CMA/106 for a perfusate rate of 0.3 μl/min) and a Harvard pump (2 μl/min). After an initial 30-min wash-out period, dialysate samples were collected every 30 min for the entire 9-h period (3-h baseline period and 6-h period for the two-step clamp).

^{1}H-NMR spectroscopy of hepatic and intramuscular triglyceride content. At 7:00 A.M on the morning after the insulin clamp, and after a 12-h fast, subjects were transported by wheelchair to the Yale Magnetic Resonance Center. Localized ^{1}H-NMR spectra of the soleus muscle were acquired on a 2.1T Biospec system (Bruker Instruments, Billerica, MA), using a coil assembly consisting of two circular hydrogen-1 coil loops (13-cm diameter each), arranged spatially to generate a quadrature field. During the measurements, the subject remained supine, and the gastrocnemius-soleus complex of the right leg was positioned within the homogeneous volume of the magnet. Scout images were acquired to position the volume of interest. Volumes of interest (15 mm × 15 mm × 25 mm) were centered within the soleus muscle and positioned to avoid vascular structures and gross adipose tissue deposits. Localized shimming in the soleus was performed using FASTERMAP (28), with typical line widths of ~10 Hz obtained. Localized proton spectra were then collected using a PRESS sequence with the following parameters: repetition time (t_R) = 3 s, echo time (t_E) = 21.1 ms, 8,192 data points over 5,000 Hz spectral width, and 128 scans. Signals in the time domain were multiplied by a Gaussian function before Fourier transformation and manual phase correction. ^{1}H resonances were assigned to water and methyl/methylene of triglycerides from their chemical shift, in agreement with Schick et al. (29), and were line fitted using the Mac-Nuts-PPC software package (Acorn NMR, Livermore, CA). Intramyocellular lipid (triglyceride) content (IMLC) and extramyocellular lipid content (EMLC) were calculated from the peak areas of intra- and extramyocellular CH_2, respectively, with respect to the water peak area, and corrected for T_1 and T_2 relaxation effects. IMLC and EMLC content were then expressed as a percentage of water content.

Localized ^{1}H-NMR spectra of the liver were obtained using a 12 × 14 cm butterfly ^{1}H observation coil placed rigidly over the lateral aspect of the abdomen. Placement of the volume of interest (15 mm × 15 mm × 15 mm) within the liver was ensured by imaging the liver with a multi-slice gradient echo sequence. Before each measurement, the water signal was optimized using a shimming procedure, where lipid signal (predominantly from subcutaneous fat) was suppressed using an inversion recovery method optimized to null the subcutaneous fat signal. Localized proton spectra were collected using a modified PRESS sequence with the following parameters: t_R = 3 s, t_E = 24.1 ms, 8,192 data points over 5,000 Hz spectral width, and 64 scans. A saturation slice centered on the chest wall was applied to prevent contamination from subcutaneous adipose tissue. The spatial position of the saturation slice was determined for each subject from the scout image. A Lorentzian filter of 5 Hz was applied before Fourier transformation and manual phase correction. Hepatic triglyceride content was calculated from the area of intrahepatic CH_2 resonance relative to the area of the water resonance, using the integration routine of Paravision software (Bruker), and then expressed as a percentage of water content.

Body composition analysis. Dual-energy X-ray absorptiometry (DEXA) scanning (Hologic QDR-4500 W; Hologic, Bedford, MA) was performed with the subject in the supine position. Fat and lean body mass in each arm and leg, the trunk, and the head were calculated assuming 17% brain fat and lean body consisting of 73% water (30).

Analyses. Plasma glucose concentrations were measured using the glucose oxidase method with a Beckman Glucose Analyzer II (Beckman Instruments, Fullerton, CA). Plasma immunoreactive insulin concentrations were measured with a double-antibody radioimmunoassay (Diagnostic System Labs, Webster, TX). Plasma fatty acid concentrations were determined using a

microfluorimetric method (31). Gas chromatography–mass spectrometry (GCMS) analysis of enrichments of [6,6-^{2}H]glucose and [1,1,2,3,3-$^2H_5$]glycerol in plasma and infusates were performed using the penta-acetate derivative of glucose and the triacetate derivative of glycerol, respectively (32). GCMS analysis was performed with a Hewlett-Packard 5971A Mass Selective Detector (Wilmington, DE) operating in the electron ionization mode. Ions with m/z 200, 201, and 202 were monitored for moles percent enrichment in glucose, and ions with m/z 145, 146, and 148 were monitored for moles percent enrichment in glycerol.

Indirect calorimetry. Basal and insulin-stimulated glucose and lipid oxidation rates were measured by the ventilated hood technique using a Deltatrack Metabolic Monitor (Sensorimedics, Anaheim, CA), as previously described (22).

Adipose tissue microdialysis. Microdialysate glycerol was measured using an enzyme-linked colorimetric determination of 0.5-μl samples by a CMA 600 microdialysis analyzer (CMA 600 Microdialysis; N. Chelmsford, MA), which has an intra-assay coefficient of variation of 2.0% and an interassay coefficient of variation of 2.0%. Ethanol concentrations in the perfusate were determined by using the automated YSI analyzer (YSI, Yellow Springs, CA).

Calculations

Insulin clamp. The rates of glucose infusion were calculated in 20-min blocks between 80 and 120 min during the low-dose insulin clamp and between 300 and 360 min of the high-dose insulin clamp. The data were corrected for urinary glucose and glucose space, averaged for each step of the clamp study, and are expressed as μmol glucose/m^2-min. Clamped glucose disposal rate (GDR_c) was calculated using the following formula:

$$GDR_c = GP_c + GIR,$$

where GP_c represents endogenous glucose production during the clamp and GIR represents the mean glucose infusion rate (mg/m^2-min) during the clamp procedure (300 to 360 min).

Basal glucose production (GP_b) was calculated using the following formula:

$$GP_b = (f/BSA) \times ([enrichment_{inf}/enrichment_{plasma}] - 1),$$

where f = basal [6,6-^{2}H]glucose infusion rate (mg/min), BSA = body surface area (m^2), $enrichment_{inf}$ = [6,6-^{2}H]glucose infusate enrichment (%), and $enrichment_{plasma}$ = steady-state basal plasma [6,6-^{2}H]glucose enrichment (%). (The term "enrichment" refers to the ratio fo glucose isotope to naturally occurring (^{12}C) glucose, expressed as a percentage.)

Clamped glucose production (GP_c) during the second step (120 mU/m^2-min) of the hyperinsulinemic-euglycemic clamp was calculated using the following formula:

$$GP_c = GIR \times ([enrichment_{inf}/enrichment_{plasma}] - 1),$$

where GIR = mean glucose infusion rate (mg/m^2-min) during the clamp procedure (300 to 360 min), $enrichment_{inf}$ = exogenous [6,6-^{2}H]glucose infusate enrichment (%), and $enrichment_{plasma}$ = steady-state clamped plasma [6,6-^{2}H]glucose enrichment (%).

Indirect calorimetry. The nonprotein respiratory quotients for 100% oxidation of fat and for oxidation of carbohydrates were 0.707 and 1.00, respectively (22). Nonoxidative glucose metabolism was calculated by subtracting the amount of glucose oxidized from the total amount of glucose infused.

Glycerol turnover. Glycerol turnover (R_a[Glycerol]) at baseline and during the two steps of the insulin clamp was calculated using the following formula:

$$R_a[Glycerol] = (f/BSA) \times ([enrichment_{inf}/enrichment_{plasma}] - 1),$$

where f = basal [$^2H_5$]glycerol infusion rate (mg/min), BSA = body surface area (m^2), $enrichment_{inf}$ = [$^2H_5$]glycerol infusate enrichment (%), and $enrichment_{plasma}$ = steady-state basal plasma [$^2H_5$]glycerol enrichment (%).

The percent glycerol suppression from adipocytes was calculated using the following formula:

$$\frac{Gly_b - Gly_{120'}}{Gly_b} \times 100\%$$

where Gly_b represents the serum glycerol concentration at baseline and $Gly_{120'}$ represents that at 120 min of the clamp.

Adipose blood flow. The change in local adipose blood flow during the hyperinsulinemic-euglycemic clamp was estimated using ethanol (ETOH) recovery rates, which are expressed as a percentage using the following formula:

$$\frac{ETOH_{out}}{ETOH_{in}} \times 100\%$$

TABLE 2
Rates of glucose and lipid oxidation before and after rosiglitazone therapy

	Before rosiglitazone	After rosiglitazone	P
Glucose oxidation			
Basal	32.4 ± 2.3	38.0 ± 5.0	0.24
Low-dose clamp	38.0 ± 2.9	46.6 ± 3.2	0.11
High-dose clamp	71.6 ± 4.7	73.5 ± 3.6	0.68
Lipid oxidation			
Basal	158.5 ± 8.8	149.7 ± 17.3	0.24
Low-dose clamp	138.9 ± 12.4	122.1 ± 8.9	0.33
High-dose clamp	67.7 ± 13.7	71.1 ± 13.1	0.59

Data are means ± SE.

where $ETOH_{in}$ represents the ethanol concentration measured in the perfusate, whereas $ETOH_{out}$ represents the ethanol concentration in the dialysate.

Statistical analyses

All statistical analyses were performed using Statview software (Abacus Concepts, Berkely, CA). All data are presented as means ± SEM. Pre- to posttherapy values are compared using a paired t test, with significance reached at $P < 0.05$.

RESULTS

Table 2 shows the changes in pertinent fasting laboratory studies before and after therapy. After 3 months of rosiglitazone treatment, mean fasting plasma glucose concentrations decreased by 12.2 ± 3.7% ($P = 0.02$), mean insulin concentrations decreased by 23.7 ± 6.9% ($P = 0.03$), and mean fasting plasma fatty acid concentrations decreased by 38.8 ± 4.6% ($P = 0.003$). Although there were no significant changes in serum hepatic transaminase levels, both alkaline phosphatase (−15.7 ± 3.8%; $P = 0.007$) and γ-glutamyl-transpeptidase (−38.8 ± 4.6%; $P = 0.001$) were significantly reduced by rosiglitazone therapy. No appreciable change in HbA_{1c} was detected, given that the baseline value reflected the degree of glycemic control achieved with the subjects' prior antidiabetic regimen, whereas the disproportionately higher fasting plasma glucose concentration likely reflected an acute deterioration in glycemic control during the washout period.

Glucose metabolism. Insulin levels were similar during both steps of the insulin clamp before and after treatment (Fig. 1). During the low-dosage clamps, the mean GIR required to maintain euglycemia increased by 68%, from 56.2 ± 4.7 to 94.2 ± 5.6 mg · m^{-2} · min^{-1} before and after

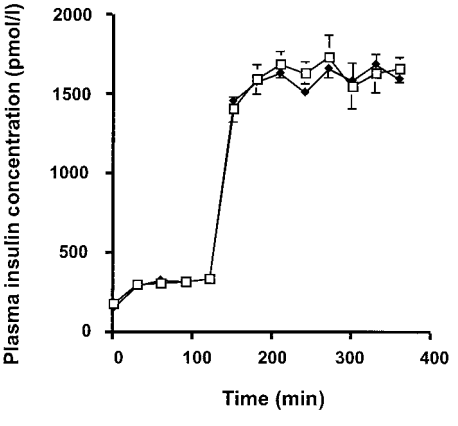

FIG. 1. Plasma insulin concentrations during the two-step hyperinsulinemic-euglycemic clamp before (□) and after (◆) rosiglitazone.

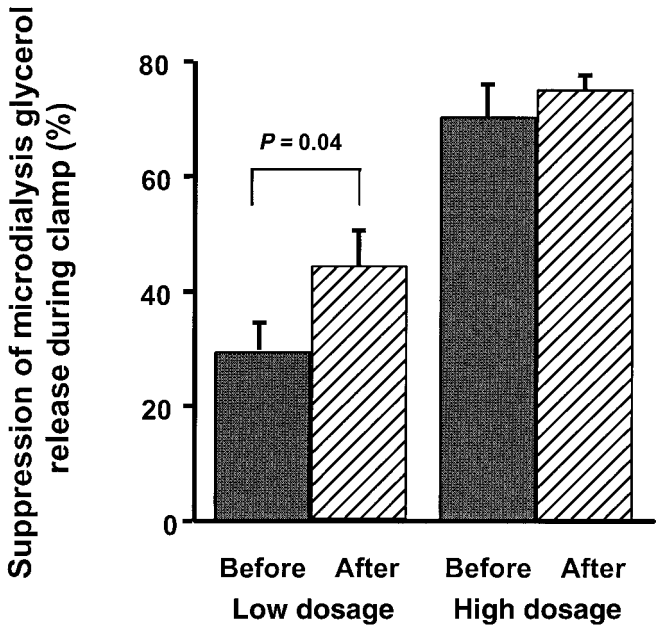

FIG. 2. Effects of 3 months of rosiglitazone treatment on insulin suppression of peripheral adipocyte lipolysis during the two-step hyperinsulinemic-euglycemic clamp.

rosiglitazone, respectively ($P < 0.0001$). During the high-dosage clamps, the mean GIR required to maintain euglycemia increased by 20%, from 296.0 ± 21.5 to 356.0 ± 24.7 mg · m^{-2} · min^{-1} before and after rosiglitazone, respectively ($P = 0.002$). The corresponding increases in the mean GDR were 119% during the low-dosage clamps (34.8 ± 9.2 vs. 76.2 ± 9.9 mg · m^{-2} · min^{-1}; $P = 0.002$) and 18% during the high-dosage clamps (340.2 ± 57.0 vs. 402.2 ± 37.1 mg · m^{-2} · min^{-1}; $P = 0.10$). Rosiglitazone had no effect on basal glucose production (101.8 vs. 93.2 mg · m^{-2} · min^{-1}; $P = 0.12$) or on the ability of insulin to suppress glucose production during the second step of the hyperinsulinemic-euglycemic clamp that was maximally suppressed in both studies.

Glucose and lipid oxidation. Basal and insulin-stimulated rates of glucose and lipid oxidation were unchanged by rosiglitazone therapy (Table 2).

Whole-body glycerol turnover. Whole-body glycerol turnover was similar before and after treatment at baseline (7.6 ± 1.2 vs. 7.6 ± 1.0 mg · m^{-2} · min^{-1}, respectively; $P = 0.99$), during the low-dosage clamp (3.2 ± 0.7 [before] vs. 2.8 ± 0.5 mg · m^{-2} · min^{-1} [after], respectively; $P = 0.34$), and during the high-dosage clamp (2.6 ± 0.4 [before] vs. 3.0 ± 0.5 mg · m^{-2} · min^{-1} [after], respectively; $P = 0.34$).

Adipocyte response to insulin. Rosiglitazone therapy led to a 52% increase in the percent suppression of glycerol release from adipocytes by insulin during the low-dosage insulin clamp (28.5 ± 6.3 vs. 43.3 ± 7.4%; $P = 0.04$). There was no significant difference in baseline microdialysis glycerol concentration or percent suppression during the high-dosage insulin clamp (Fig. 2). Relative changes in adipocyte blood flow were estimated by measuring the ratio of $ETOH_{out}$ to $ETOH_{in}$, representing the concentration of ethanol in the dialysate versus that in the perfusate during the microdialysis procedure, as previously described and validated (26,27). A lower ratio indicates decreased ETOH recovery and therefore an increase in local blood flow. There was no effect of rosiglitazone on the percent change in ETOH recovery during the low-dosage clamp (4.8 ± 2.3 [before] vs. 5.0 ± 4.7 [after]; $P = 0.96$).

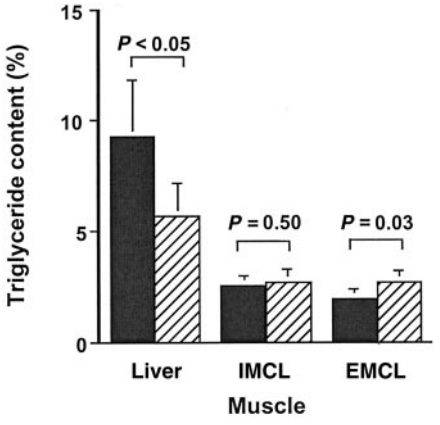

FIG. 3. Effects of 3 months of rosiglitazone treatment on hepatic triglyceride, IMLC, and EMLC content. ■, before rosiglitazone; ▨, after rosiglitazone.

Hepatic lipid content. The 3 months of rosiglitazone treatment caused a 39% decrease in hepatic triglyceride content (9.3 ± 2.5 vs. 5.7 ± 1.5%; $P < 0.05$) (Fig. 3).

Muscle lipid content. The IMLC did not change significantly after 3 months of rosiglitazone therapy (2.5 ± 0.4 vs. 2.7 ± 0.6%; $P = 0.50$). In contrast, the EMLC increased by 39%, from 1.9 ± 0.50 to 2.7 ± 0.5% ($P = 0.03$) after 3 months of rosiglitazone treatment (Fig. 3).

Body composition. There were no detectable changes in body weight or body composition as assessed by DEXA between baseline recordings and at the conclusion of 3 months of rosiglitazone therapy: body weight 92.3 ± 3.0 vs. 93.9 ± 5.7 kg, $P = 0.34$; lean body mass 61.3 ± 3.4 vs. 59.9 ± 2.5 kg, $P = 0.98$; and percent body fat 29.9 ± 3.6 vs. 33.1 ± 4.5%; $P = 0.78$.

DISCUSSION

The 3 months of rosiglitazone treatment resulted in a significant improvement in insulin-stimulated glucose disposal that could mostly be attributed to an increase in nonoxidative glucose metabolism. These results are similar to the results from previous hyperinsulinemic-euglycemic clamp studies examining troglitazone treatment in patients with type 2 diabetes (3–5). This improvement in insulin responsiveness was associated with a marked reduction in hepatic triglyceride content and an increase in extramyocellular triglyceride content. Furthermore, we found that rosiglitazone treatment resulted in a significant improvement in peripheral adipocyte insulin responsiveness, as reflected by an increase in insulin suppression of peripheral adipocyte lipolysis and decreased plasma fatty acid concentrations. Overall, these results are consistent with the hypothesis that TZDs improve insulin sensitivity in patients with type 2 diabetes by activating PPAR-γ in peripheral adipocytes and promoting adipocyte differentiation (33,34). This results in an increase in smaller and more insulin-responsive adipocytes, which in turn leads to lower circulating plasma fatty acid concentrations and a redistribution of lipid (and intracellular fatty acid metabolites) from liver and muscle to peripheral adipocytes.

Consistent with this theory are the recent findings that rosiglitazone's antidiabetic effect is severely curtailed in an insulin-resistant transgenic mouse model of lipoatrophy (35).

The marked reduction that we observed in hepatic triglyceride content was associated with decreases in serum alkaline phosphatase and γ-glutamyl-transpeptidase, both markers of hepatic infiltration that are frequently elevated in steatohepatitis. These data suggest that TZD therapy may be useful in patients with nonalcoholic steatohepatitis, which has been associated with insulin resistance, obesity, and diabetes. Specific studies of patients with more severe fatty infiltration may further clarify this issue.

Surprisingly, we found that rosiglitazone caused no significant decrease in intramyocellular triglyceride content, despite a significant improvement in muscle insulin sensitivity. In contrast, Ye et al. (36) have recently reported that pioglitazone decreases triglyceride and fatty acyl CoA content in skeletal muscle of Zucker rats. Although species differences might explain these discrepant results, it is more likely that intramuscular triglyceride content is just a marker for another intramyocellular fatty acid metabolite, such as fatty acyl CoA, that is actually responsible for events leading to decreased insulin receptor substrate-1–associated phosphoinositol 3-kinase activity (34).

In contrast, rosiglitazone treatment caused a significant increase in EMCL, a finding that is consistent with rosiglitazone's effects in promoting adipocyte differentiation and suggests that extramyocellular adipocytes behave similarly to peripheral adipocytes in response to TZDs. These findings are consistent with the results of Kelley et al. (37), who found that 3 months of troglitazone therapy in subjects with type 2 diabetes improved fasting plasma glucose concentrations while increasing total body fat mass. Body composition analysis by computed tomography revealed that this increase was exclusively attributable to an increase in peripheral adiposity, while visceral fat stores decreased. Similar results have been achieved by other groups using troglitazone (38–41) and pioglitazone (42) in patients with type 2 diabetes and lipodystrophy (43). This redistribution of body fat may result from the predilection for certain PPAR-γ agonists to induce pre-adipocyte differentiation in subcutaneous rather than visceral fat depots (45).

It is also possible that rosiglitazone improves insulin sensitivity in type 2 diabetes by altering the concentrations of certain adipocyte-derived hormones, such as leptin (6), TNF-α, adiponectin (7), or resistin (9). With regard to leptin, we found no significant effects of rosiglitazone on fasting or insulin-stimulated leptin concentrations. Previous in vitro and in vivo studies on the effects of TZDs on leptin production by adipocytes have yielded conflicting results (45–49). Nolan et al. (45) showed that co-incubation of adipocytes with troglitazone abolished the usual twofold increase in insulin-stimulated leptin production in vitro. In contrast rosiglitazone had no effect on plasma leptin concentrations in obese Zucker rats (46). In obese, nondiabetic human subjects, troglitazone caused no change in leptin levels, but has been shown to decrease leptin concentrations in diabetic subjects (47,48). Based on our results, an alteration in circulating leptin concentrations does not appear to play a major role in mediating the insulin-sensitizing effects of rosiglitazone. The effects of rosiglitazone on other circulating fat-derived factors, such as resistin, TNF-α, and adiponectin, which may modify insulin sensitivity in type 2 diabetic subjects, remain to be determined.

In summary, we found that 3 months of rosiglitazone treatment resulted in an improvement in an insulin responsiveness in type 2 diabetic subjects that was associated with a marked reduction in hepatic triglyceride content and an increase in EMLC. These changes were associated with an enhancement of insulin's ability to suppress peripheral adipocyte lipolysis. Overall, these results support the hypothesis that TZDs enhance insulin sensitivity in patients with type 2 diabetes by promoting increased insulin sensitivity in peripheral adipocytes, which results in a redistribution of intracellular lipid from insulin responsive organs into adipocytes.

ACKNOWLEDGMENTS

This work was supported by U.S. Public Health Service grants R01-DK-49230, P30-DK-45735, and M01-RR-00125; a U.S. Public Health Service K-23 award (K.F.P.); and a grant from Glaxo Smith-Kline (K.F.P.).

The authors thank the staff of the Yale University–New Haven Hospital GCRC for expert assistance with these studies.

REFERENCES

1. Day C: Thiazolidinediones: a new class of antidiabetic drugs. *Diabet Med* 16:179–192, 1999
2. Tontonoz P, Hu E, Spiegelman BM: Regulation of adipocyte gene expression and differentiation by peroxisome proliferator activated receptor gamma. *Curr Opin Genet Dev* 5:571–576, 1995
3. Maggs DG, Buchanan TA, Burant CF, Cline G, Gumbiner B, Hsueh WA, Inzucchi S, Kelley D, Nolan J, Olefsky JM, Polonsky KS, Valiquett TR, Shulman GI: Metabolic effects of troglitazone monotherapy in type 2 diabetes mellitus: a randomized, double-blind, placebo-controlled trial. *Ann Intern Med* 128:176–185, 1998
4. Inzucchi SE, Maggs DG, Spollett GR, Page SL, Rife FS, Walton V, Shulman GI: Efficacy and metabolic effects of metformin and troglitazone in type II diabetes mellitus. *N Engl J Med* 338:867–872, 1998
5. Petersen KF, Krssak M, Inzucchi S, Cline GW, Dufour S, Shulman GI: Mechanism of troglitazone action in type 2 diabetes. *Diabetes* 49:827–831, 2000
6. Shimomura H, Hammer RE, Ikemoto S, Brown MS, Goldstein JL: Leptin reverses insulin resistance and diabetes mellitus in mice with congenital lipodystrophy. *Nature* 401:73–76, 1999
7. Yamauchi T, Kamon J, Waki H, Terauchi Y, Kubota N, Hara K, Mori Y, Ide T, Murakami K, Tsuboyama-Kasaoka N, Ezaki O, Akanuma Y, Gavrilova O, Vinson C, Reitman ML, Kagechika H, Shudo K, Yoda M, Nakano Y, Tobe K, Nagai R, Kimura S, Tomita M, Froguel P, Kadowaki T: The fat-derived hormone adiponectin reverses insulin resistance associated with both lipoatrophy and obesity. *Nat Med* 7:941–946, 2001
8. Hotamisligil GS, Shargill NS, Spiegelman BM: Adipose expression of tumor necrosis factor-alpha: direct role in obesity-linked insulin resistance. *Science* 259:87–91, 1993
9. Steppan CM, Bailey ST, Bhat S, Brown EJ, Banerjee RR, Wright CM, Patel HR, Ahima RS, Lazar MA: The hormone resistin links obesity to diabetes. *Nature* 409:307–312, 2001
10. Boden G, Chen X: Effects of fat on glucose uptake and utilization in patients with non-insulin-dependent diabetes. *J Clin Invest* 96:1261–1268, 1995
11. Roden M, Price TB, Perseghin G, Petersen KF, Rothman DL, Cline GW, Shulman GI: Mechanism of free fatty acid-induced insulin resistance in humans. *J Clin Invest* 97:2859–2865, 1996
12. Dresner A, Laurent D, Marcucci M, Griffin ME, Dufour S, Cline GW, Slezak LA, Andersen DK, Hundal RS, Rothman DL, Petersen KF, Shulman GI:

Effects of free fatty acids on glucose transport and IRS-1-associated phosphatidylinositol 3-kinase activity. *J Clin Invest* 103:253–259, 1999
13. Griffin ME, Marcucci MJ, Cline GW, Bell K, Barucci N, Lee D, Goodyear LJ, Kraegen EW, White MF, Shulman GI: Free fatty acid-induced insulin resistance is associated with activation of protein kinase C theta and alterations in the insulin signaling cascade. *Diabetes* 48:1270–1274, 1999
14. Perseghin G, Scifo P, De Cobelli F, Pagliato E, Battezzati A, Arcelloni C, Vanzulli A, Testolin G, Pozza G, Del Mascio A, Luzi L: Intramyocellular triglyceride content is a determinant of in vivo insulin resistance in humans. *Diabetes* 48:1600–1606, 1999
15. Kim JK, Gavrilova O, Chen Y, Reitman ML, Shulman GI: Mechanism of insulin resistance in A-ZIP/F-1 fatless mice. *J Biol Chem* 275:8456–8460, 2000
16. Kim JK, Fillmore JJ, Chen Y, Yu C, Moore IK, Pypaert M, Lutz EP, Kako Y, Velez-Carrasco W, Goldberg IJ, Breslow JL, Shulman GI: Tissue-specific overexpression of lipoprotein lipase causes tissue-specific insulin resistance. *Proc Natl Acad Sci U S A* 98:7522–7527, 2001
17. Krssak M, Falk Petersen K, Dresner A, DiPietro L, Vogel SM, Rothman DL, Roden M, Shulman GI: Intramyocellular lipid concentrations are correlated with insulin sensitivity in humans: a ^{1}H NMR spectroscopy study. *Diabetologia* 42:113–116, 1999
18. Pan DA, Lillioja S, Kriketos AD, Milner MR, Baur LA, Bogardus C, Jenkins AB, Storlien LH: Skeletal muscle triglyceride levels are inversely related to insulin action: *Diabetes* 46:983–988, 1997
19. Jucker BM, Cline GW, Barucci N, Shulman GI: Differential effects of safflower oil versus fish oil feeding on insulin-stimulated glycogen synthesis, glycolysis, and pyruvate dehydrogenase flux in skeletal muscle: a 13C nuclear magnetic resonance study *Diabetes* 48:134–140, 1999
20. Laybutt DR, Schmitz-Peiffer C, Saha AK, Ruderman NB, Biden TJ, Kraegen EW: Muscle lipid accumulation and protein kinase C activation in the insulin-resistant chronically glucose-infused rat. *Am J Physiol* 277: E1070–E1076, 1999
21. Ryysy L, Hakkinen AM, Goto T, Vehkavaara S, Westerbacka J, Halavaara J, Yki-Jarvinen H: Hepatic fat content and insulin action on free fatty acids and glucose metabolism rather than insulin absorption are associated with insulin requirements during insulin therapy in type 2 diabetic patients. *Diabetes* 49:749–758, 2000
22. Lusk G: Animal calorimetry: analysis of the oxidation of mixtures of carbohydrates and fat. A correction. *J Biol Chem* 59:41–42, 1924
23. Lafontan M, Arner P: Application of in situ microdialysis to measure metabolic and vascular responses in adipose tissue. *Trends Pharmacol Sci* 17:309–313, 1996
24. Tossman U, Ungerstedt U: Microdialysis in the study of extracellular levels of amino acids in the rat brain. *Acta Physiol Scand* 128:9–14, 1986
25. Arner P, Bulow J: Assessment of adipose tissue metabolism in man: comparison of Fick and microdialysis techniques. *Clin Sci* 82:247–256, 1993
26. Hickner RC, Rosdahl H, Borg I, Ungerstedt U, Jorfeldt L, Henricksson J: Ethanol may be used with the microdialysis technique to monitor blood flow changes in skeletal muscle: dialysate glucose concentrations is bloodflow dependent. *Acta Physiol Scand* 146:87–97, 1992
27. Fellander G, Linde B, Bolinder J: Evaluation of the microdialysis ethanol technique for monitoring of subcutaneous adipose tissue blood flow in humans. *Int J Obes Relat Metab Disord* 20:220–226, 1996
28. Shen J, Rycyna RE, Rothman DL: Improvements on an in vivo automatic shimming method [FASTERMAP]. *Magn Reson Med* 38:834–839, 1997
29. Schick F, Eismann B, Jung WI, Bongers H, Bunse M, Lutz O: Comparison of localized proton NMR signals of skeletal muscle and fat tissue in vivo: two lipid compartments in muscle tissue. *Magn Reson Med* 29:158–167, 1993
30. Brozek JF, Grande JT, Andersen T, Keys A: Densitometric analysis of body composition: revision of some quantitative assumptions. *Ann N Y Acad Sci* 110:113–140, 1963
31. Miles J, Glasscock R, Aikens J, Gerich J, Haymond M: A microfluorometric method for the determination of free fatty acids in plasma. *J Lipid Res* 24:96–99, 1983
32. Wolfe RR: *Radioactive and Stable Isotope Tracers in Biomedicine: Principles and Practice of Kinetic Analysis*. New York, Wiley, 1992
33. Okuno A, Tamemoto H, Tobe K, Ueki K, Mori Y, Iwamoto K, Umesono K, Akanuma Y, Fujiwara T, Horikoshi H, Yazaki Y, Kadowaki T: Troglitazone increases the number of small adipocytes without the change of white adipose tissue mass in obese Zucker rats. *J Clin Invest* 101:1354–1361, 1998
34. Shulman GI: Cellular mechanisms of insulin resistance. *J Clin Invest* 106:171–176, 2000
35. Chao L, Marcus-Samuels B, Mason MM, Moitra J, Vinson C, Arioglu E, Gavrilova O, Reitman ML: Adipose tissue is required for the antidiabetic, but not for the hypolipidemic, effect of thiazolidinediones. *J Clin Invest* 106:1221–1228, 2000
36. Ye JM, Doyle PJ, Iglesias MA, Watson DG, Cooney GJ, Kraegen EW: Peroxisome proliferator-activated receptor (PPAR)-alpha activation lowers muscle lipids and improves insulin sensitivity in high fat-fed rats: comparison with PPAR-gamma activation. *Diabetes* 50:411–417, 2001
37. Kelly IE, Han TS, Walsh K, Lean ME: Effects of a thiazolidinedione compound on body fat and fat distribution of patients with type 2 diabetes. *Diabetes Care* 22:288–293, 1999
38. Mori Y, Murakawa Y, Okada K, Horikoshi H, Yokoyama J, Tajima N, Ikeda Y: Effect of troglitazone on body fat distribution in type 2 diabetic patients. *Diabetes Care* 22:908–912, 1999
39. Kawai T, Takei I, Oguma Y, Ohashi N, Tokui M, Oguchi S, Katsukawa F, Hirose H, Shimada A, Watanabe K, Saruta T: Effects of troglitazone on fat distribution in the treatment of male type 2 diabetes. *Metabolism* 48:1102–1107, 1999
40. Akazawa S, Sun F, Ito M, Kawasaki E, Eguchi K: Efficacy of troglitazone on body fat distribution in type 2 diabetes. *Diabetes Care* 23:1067–1071, 2000
41. Katoh S, Hata S, Matsushima M, Ikemoto S, Inoue Y, Yokoyama J, Tajima N: Troglitazone prevents the rise in visceral adiposity and improves fatty liver associated with sulfonylurea therapy: a randomized controlled trial. *Metabolism* 50:414–417, 2001
42. Miyazaki Y, Mahankali A, Matsuda M, Mahankali S, Cusi K, Mandarino J, Defronzo RA: Relationship between visceral fat and enhanced peripheral/hepatic insulin sensitivity after pioglitazone in type 2 diabetes. *Diabetes* 50 (Suppl. 2):A126, 2001
43. Arioglu E, Duncan-Morin J, Sebring N, Rother KI, Gottlieb N, Lieberman J, Herion D, Kleiner DE, Reynolds J, Premkumar A, Sumner AE, Hoofnagle J, Reitman ML, Taylor SI: Efficacy and safety of troglitazone in the treatment of lipodystrophy syndromes. *Ann Intern Med* 133:263–274, 2000
44. Adams M, Montague CT, Prins JB, Holder JC, Smith SA, Sanders L, Digby JE, Sewter CP, Lazar MA, Chatterjee VK, O'Rahilly S: Activators of peroxisome proliferator-activated receptor gamma have depot-specific effects on human preadipocyte differentiation. *J Clin Invest* 100:3149–3153, 1997
45. Nolan JJ, Olefsky JM, Nyce MR, Considine RV, Caro JF: Effect of troglitazone on leptin production: studies in vitro and in human subjects. *Diabetes* 45:1276–1278, 1996
46. Wang Q, Dryden S, Frankish HM, Bing C, Pickavance L, Hopkins D, Buckingham R, Williams G: Increased feeding in fatty Zucker rats by the thiazolidinedione BRL 49653 (rosiglitazone) and the possible involvement of leptin and hypothalamic neuropeptide Y. *Br J Pharmacol* 122:1405–1410, 1997
47. Shimizu H, Tsuchiya T, Sato N, Shimomura Y, Kobayashi I, Mori M: Troglitazone reduces leptin concentration but increases hunger in NIDDM patients. *Diabetes Care* 21:1470–1474, 1998
48. Mantzoros CS, Dunaif A, Flier JS: Leptin concentrations in the polycystic ovary syndrome. *J Clin Endocrinol Metab* 82:1687–1691, 1997